Intracrystalline and Electronic Structures of Copper(II) Complexes Stabilized in Two-Dimensional Aluminosilicate

Jin-Ho Choy*

Department of Chemistry, Center for Molecular Catalysis (CMC), College of Natural Sciences, Seoul National University, Seoul 151-742, Korea

Dong-Kuk Kim

Department of Chemistry, Kyungpook National University, Taegu, 702-701, Korea

Jung-Chul Park

Department of Chemistry, College of Natural Sciences, Pusan Women's University, Pusan 616-736, Korea

Sung-Nak Choi and Young-Jin Kim

Department of Chemistry, College of Natural Sciences, Pusan National University, Pusan 609-735, Korea

Received May 28, 1996[⊗]

X-ray absorption spectroscopic studies at the Cu K-edge have been performed for $[Cu(en)_2]^{2+}$, $[Cu(cyclam)]^{2+}$, and their intercalated forms of two-dimensional layer silicate to examine how the structural and electronic modifications influence the stabilization of copper complexes in the charged interlayer space. According to the EXAFS analysis, copper complex ions in the layer silicate are stabilized at the center of the siloxane ring, and negatively charged layers are likely to act as axial counteranions. It is spectroscopically confirmed that the covalent bonding character between copper and ligand is enhanced by the intercalation into the silicate layers, depending upon the kind of ligands. There is a good linear relationship between the shoulder peak position of Cu K-edge XANES spectra and d−d transition band position of UV−visible spectra, which means that the former reflects the ligand-to-metal charge transfer effect.

Introduction

Various kinds of transition metal complexes with polyaza macrocyclic ligands[1−7] have received much attention due to their significant catalytic activities in electrochemical, biological, and photobiological processes. Such complexes have been successfully intercalated into the charged layer of host structures such as clay mineral by ion-exchange reaction,[8−17] and these intercalates have often exhibited efficient biomimetic catalytic properties comparable to those of the homogeneous solution containing the same amount of the metal complex.[18,19] In addition, many transition metal cationic porphyrins have been known to be stable against demetalation on clay surfaces,[15,17,20] and from several studies, it has been pointed out that the complex stability on clay surfaces may be different from that in solution.[20−24] It is expected that the electronic configuration, mobility, and orientation of the complex could be altered in the interlayer surface of clays. Therefore, the characterization

* To whom correspondence should be addressed.

[⊗] Abstract published in *Advance ACS Abstracts,* December 1, 1996.

(1) Abb, F.; Santis, G. D.; Fabbrizzi, L.; Licchelli, M.; Lanfredi, A. M. M.; Pallavicini, P.; Poggi, A.; Ugozzoli, F. *Inorg. Chem.* **1994**, *33*, 1366.
(2) Zagal, J. H. Coord. *Chem. Rev.* **1992**, *119*, 89.
(3) Mártire, D. O.; Jux, N.; Aramendía, P. F.; Negri, R. M.; Lex. J.; Braslavsky, S. E.; Schaffner, K.; Vogel, E. *J. Am. Chem. Soc.* **1992**, *114*, 9969.
(4) Luckay, R. C.; Hancock, R. D. *J. Chem. Soc., Dalton Trans.* **1991**, 1491.
(5) Clewly, R. G.; Slebocka-Jilk, H.; Brown, R. S. *Inorg. Chim. Acta* **1989**, *157*, 233.
(6) Morgan, B.; Dolphin, D. *Struct. Bonding* **1987**, *64*, 116.
(7) Fabbrizzi, L.; Poggi, A.; Zanello, P. *J. Chem. Soc., Dalton Trans.* **1983**, 2191.
(8) Meister, A.; Takano, N.; Chuard, T.; Graf, M.; Bernauer, K.; Steoeckli-Evans, H.; Süss-Fink, G. *Z. Anorg. Allg. Chem.* **1995**, *621*, 117.
(9) Ukrainczyk, L.; Chibwe, M.; Pinnavaia, T. J.; Boyd, S. A. *J. Phys. Chem.* **1994**, *98*, 2668.
(10) Holtz, M.; Park, T. -R.; Amarasekera, J.; Solin, S. A.; Pinnavaia, T. J. *J. Chem. Phys.* **1994**, *100*, 3346.
(11) Kijima, T.; Sakaguchi, K.; Ohe, K. *Bull. Chem. Soc. Jpn.* **1994**, *67*, 1281.
(12) Carrado, K. A.; Forman, J. E.; Botto, R. E.; Winans, R. E. *Chem. Mater.* **1993**, *5*, 472.
(13) Rao, Y. V. S.; Rani, S. S.; Choudary, B. M. *J. Mol. Catal.* **1992**, *75*, 141.
(14) Taniguchi, M.; Yamagishi, A.; Iwamoto, T. *Inorg. Chem.* **1991**, *30*, 2462.
(15) Carrado, K. A.; Thiyagarajan, P.; Winans, R. E.; Botto, R. E. *Inorg. Chem.* **1991**, *30*, 794.
(16) Yamagishi, A. *J. Coord. Chem.* **1987**, *16*, 131.
(17) Giannelis, E. P. *Chem. Mater.* **1990**, *2*, 627.
(18) Chibwe, M.; Pinnavaia, T. J. *J. Chem. Soc., Chem. Commun.* **1993**, 278.
(19) Caillon, L.; Bedioui, F.; Battioni, P.; Devynck, J. *J. Mol. Catal.* **1993**, *78*, L23.
(20) Carrado, K. A.; Winans, R. E. *Chem. Mater.* **1990**, *2*, 328.
(21) Schoonheydt, R. A.; Pelgrims, J. *J. Chem. Soc., Faraday Trans. 2* **1983**, *79*, 1169.
(22) Maes, A.; Schoonheydt, R. A.; Cremers, A.; Uytterhoeven, J. B. *J. Phys. Chem.* **1980**, *84*, 2795.
(23) Maes, A.; Peigneur, P.; Cremers, A. *J. Chem. Soc., Faraday Trans. 1* **1978**, *74*, 182.
(24) Velghe, F.; Schoonheydt, R. A.; Uytterhoeven, J. B.; Peigneur, P.; Lunsford, J. H. *J. Phys. Chem.* **1977**, *81*, 1187.

S0020-1669(96)00631-3 CCC: $14.00 © 1997 American Chemical Society

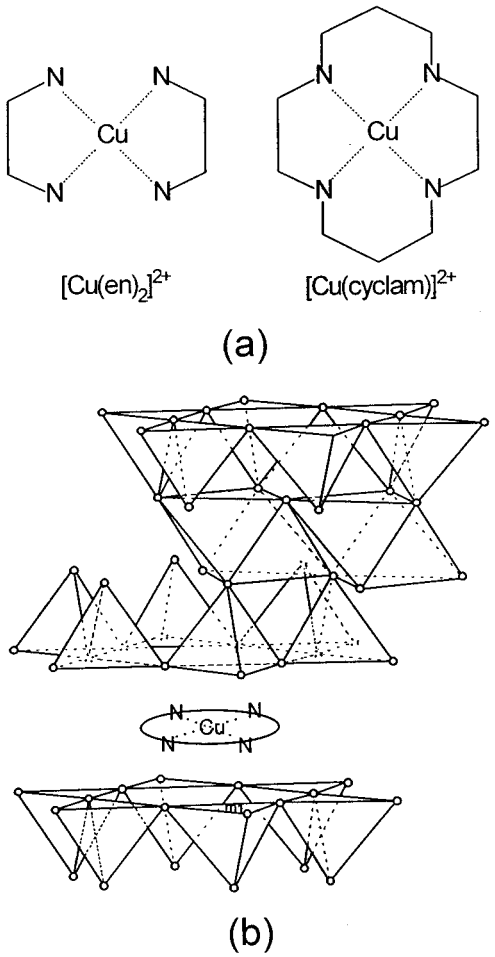

Figure 1. Schematic representations of copper(II) complex cations (a) and their intercalates (b) for the present study, where m1 indicates the site located between triangular basal oxygen atoms of the SiO_4 tetrahedra.

of the chemical bonding nature as well as the local structure of transition metal ion within the charged layers has been one of the most attractive research problems. However, the insufficiency in numbers and intensities of the observed (00l) reflections due to their lower dimensionality might make it impossible for the powder X-ray diffraction method to determine directly the geometry and ligand environment of the metal complex ion intercalated into clay material. In addition, even though nearly all the conceivable permutations have been proposed by means of spectroscopies such as IR,[8,25,26] UV−visible,[15,27] and EPR,[9,17,28,29] it is still unclear how the intercalation of metal complex into the charged layer affects the changes in coordination of a transition metal and bonding character. In these points of view, X-ray absorption spectroscopy would be a useful tool to probe the metal ions absorbed in the interlayer,[30−39] because of its peculiar property of being sensitive to both structural and electronic evolutions in a specific atom due to its element selectivity and no requirement of long-range order in the crystal structure.

Table 1. Chemical Analyses of C, H, and N for Synthetic $[Cu(en)_2](ClO_4)_2$ and $[Cu(cyclam)](ClO_4)_2$[a]

compound	C	H	N
$[Cu(en)_2](ClO_4)_2$	12.79 (12.83)	2.06 (2.14)	14.71 (14.95)
$[Cu(cyclam)](ClO_4)_2$	25.78 (25.95)	5.24 (5.19)	12.14 (12.01)

[a] Values in parentheses indicate those calculated for ideal compositions.

In the present work, two model Cu(II) complexes (Figure 1) of $[Cu(en)_2]^{2+}$ (en = ethylenediamine), and $[Cu(cyclam)]^{2+}$ (cyclam = 1,4,8,11-tetraazacyclotetradecane) have been examined to study how the local structural change and the crystal field effects could be associated with the evolution of electronic environment around the copper ion upon the intercalation of those complexes into montmorillonite by means of the Cu K-edge EXAFS and XANES as well as powder XRD and UV−visible spectroscopy, and these intercalates have been carefully compared with those of their free Cu(II) complexes as well as the Cu(II) ion-exchanged montmorillonite.

Experimental Section

Sample Preparation. The ligands, en and cyclam were used as received from Fluka Co. All solvents were of special grade and were dried, distilled, and rigorously degassed before use. All the reactions were carried out under argon with standard Schlenk techniques unless otherwise stated. For the synthesis of bis(ethylenediamine) copper(II) perchlorate ($[Cu(en)_2](ClO_4)_2$), the ethylenediamine (1.3 mL, 20 mmol) was added to the solution of copper(II) perchlorate hexahydrate (3.705 g, 10 mmol) dissolved in absolute methanol/trimethylorthoformate (5:1). The mixture was refluxed for several hours, and cooled down to room temperature. The precipitates were filtered, and then the crude products were recrystallized in hot ethanol. The purple complex obtained was washed with cold methanol, and then dried in vacuum. For the synthesis of 1,4,8,11-tetraazacyclotetradecane copper(II) perchlorate ($[Cu(cyclam)](ClO_4)_2$), a solution of copper(II) perchlorate hexahydrate (3.705 g, 10 mmol) in absolute ethanol/trimethyl orthoformate (5:1) was slowly added to a solution of 1,4,8,11-tetraazacyclotetradecane (2.0 g, 10 mmol) in ethanol (40 mL)/acetonitrile (60 mL), and the mixture solution was refluxed at 80 °C overnight in an argon atmosphere. The purple mixture was filtered on warming. The filtrate was cooled, and then the purple precipitate was isolated by filtration, washed with cold ethanol, and dried in vacuum. Chemical analyses for both products, bis(ethylenediamine) copper(II) perchlorate and 1,4,8,11-tetraazacyclotetradecane copper(II) perchlorate, are presented in Table 1. Quantitative elemental analyses were completed on the thermal conductivity detector with an EA 1108 elemental analyzer (Fisons Co.) Microanalyses for carbon, hydrogen, and nitrogen were obtained under following conditions: 100 mL/min (±10%) carrier gas (He) flow rate, furnace temperature of 1020 °C, oven temperature of 60 °C, and sample delay time of 8−15 s, depending on the carrier gas flow rate used. For the ion-exchange-type intercalation reaction, montmorillonite (Junsei Chemical Co., Ltd.) was at first converted into the sodium form by treating it with 1 N NaCl solution, and the excess salt was then removed by dialysis. These sodium-saturated samples

(25) Kaneyoshi, M.; Yamagishi, A.; Tanaguchi, M.; Aramata, A. *Clays Clay Miner.* **1993**, *41*, 1.
(26) Pusino, A.; Micera, G.; Gessa, C. *Clays Clay Miner.* **1991**, *39*, 50.
(27) Velghe, F.; Schoonheydt, R. A.; Uytterhoeven, J. B. *Clays Clay Miner.* **1977**, *25*, 375.
(28) Pusino, A.; Cera, G. M.; Premoli, A.; Gessa, C. *Clays Clay Miner.* **1989**, *37*, 377.
(29) Rupert, J. P. *J. Phys. Chem.* **1973**, *77*, 784.
(30) Choy, J. H.; Yoon, J. B.; Kim, D. K.; Hwang, S. H. *Inorg. Chem.* **1995**, *34*, 6524.
(31) O'day, P. A.; Brown, G. E., Jr.; Parks, G. A. *J. Colloid Interface Sci.* **1994**, *165*, 269.
(32) Charlet, L.; Manceau, A. *Geochim. Cosmochim. Acta* **1994**, *58*, 2577.
(33) Carrado, K. A.; Wasserman, S. R. *J. Am. Chem. Soc.* **1993**, *115*, 3394.
(34) Trillo, J. M.; Alba, M. D.; Alvero, R.; Castro, M. A.; Muñoz, A.; Poyato, J.; Tobías, M. M.; Lagaly, G. *Solid State Ionics* **1993**, *63−65*, 457.
(35) Dent, A. J.; Ramsay, J. D. F.; Swanton, S. W. *J. Colloid Interface Sci.* **1992**, *150*, 45.
(36) Bornholdt, K.; Corker, J. M.; Evans, J.; Rummey, J. M. *Inorg. Chem.* **1991**, *30*, 1.
(37) Choi, E. Y.; Nam, I. S.; Kim, Y. G.; Chung, J. S.; Lee, J. S. *J. Mol. Catal.* **1991**, *69*, 247.
(38) Jones, D. J.; Rozlère, J. *J. Chem. Soc., Faraday Trans.* **1991**, *87*, 3077.
(39) Ildefonse, P.; Manceau, A.; Prost, D.; Groke, A. C. T. *Clays Clay Miner.* **1986**, *34*, 338.

were then fractionated by Stoke's law with a particle size below 2 μm. For the formation of montmorillonite−copper(II) complexes, montmorillonite (sample weight ∼1 g) was immersed into bis(ethylenediamine) copper(II) perchlorate (sample weight ∼1 g) solution and 1,4,8,11-tetraazacyclotetradecane copper(II) perchlorate (sample weight ∼1 g) at 65 °C for 24 h, respectively. After decanting supernatant liquid and washing, each sample was reacted again for the same period. An ultrasonic cleaner was used intermediately in order to perform the homogeneous ion-exchange reaction. For comparison, the cupric ion-exchanged montmorillonite was prepared by treating it with 1 N $CuCl_2$ solution. The ion-exchanged clays were centrifuged until the clay suspension gave a colorless supernatant, indicating that the copper complex had been completely exchanged. The products were washed three times with deionized water to remove excess salt and dried under high vacuum ($<10^{-5}$ Torr) at 65 °C for 24 h and then freeze-dried at −50 °C for 24 h ($<10^{-5}$ Torr).

Powder XRD and UV−Visible Spectroscopy. X-ray diffraction measurements on powdered clay products were performed with a Rigaku diffractometer with Ni-filtered Cu Kα radiation. UV−visible spectra were recorded at room temperature on a Shimadzu UV-265 spectrophotometer.

X-ray Absorption Spectroscopy. X-ray absorption spectroscopic measurements were carried out with synchrotron radiation by using the EXAFS facilities installed at the beam line 10B of the Photon Factory, the National Laboratory for High Energy Physics (Tsukuba), operated at 2.5 GeV with ∼260−370 mA of stored current. Samples were ground into a fine powder in a mortar and then spread uniformly onto an adhesive tape, which was folded into layers to obtain an optimum absorption jump ($\Delta\mu t \approx 1$) enough to be free from the thickness and pinhole effects. All the data were recorded in a transmission mode at room temperature, using a Si(311) channel-cut monochromator. The intensities of incident and transmitted beams were measured with N_2- and (25% Ar/75% N_2)−filled ionization chambers, respectively. The spectrometer energy resolution was ∼0.1 eV. To ensure the spectral reliability, much care has been made to evaluate the stability of the energy scale by monitoring the copper metal spectrum for each measurement, and thus edge positions were reproducible to better than 0.05 eV.

XANES and EXAFS Data Analysis. The data analyses for experimental spectra were performed by the standard procedure as previously described. Photon energies of all XANES spectra were calibrated by the first absorption peak of copper metal foil spectrum, located at 8980.3 eV. The inherent background was removed from all spectra by fitting a straight line to the pre-edge region and subtracting this fitted background from the entire spectrum. The resulting spectra were normalized by adjusting an edge jump to 1.

For the EXAFS analysis, the absorption spectrum for the isolated atom, $\mu_0(E)$, was approximated by some cubic splines ($\mu(E)$). The EXAFS function, $\chi(E)$, was obtained as $\chi(E) = \{\mu(E) - \mu_0(E)\}/\mu_0(E)$. Further analysis was performed in a k space, where the photoelectron wave vector k is defined by $\{(8\pi^2 m_e/h^2)(E - E_0)\}^{1/2}$, where m_e is the electron mass, h is Planck constant, E is the photon energy, and E_0 is the threshold energy of photoelectron at $k = 0$. The resulting EXAFS spectra were k^3 weighted in order to compensate for the attenuation of EXAFS amplitude at high k and then Fourier transformed in the range of ~ 2 Å$^{-1} \le k \le \sim 13$ Å^{-1} with a Hanning apodization function.

In order to determine the structural parameters, a nonlinear least-squares curve fitting was performed in the R space of the Fourier transform (FT), using a UWXAFS code[40] according to the following EXAFS formula.

$$\chi(k) = -S_0^2 \sum_i \frac{N_i}{kR_i^2} F_i(k) \exp\{-2\sigma_i^2 k^2\} \exp\{-2R_i/\lambda(k)\} \times \sin\{2kR_i + \phi_i(k)\}$$

The backscattering amplitude, $F_i(k)$, the total phase shift, $\phi_i(k)$, and the photoelectron mean free path, $\lambda(k)$, have been theoretically calculated for all scattering paths including multiple scattering by a curved wave *ab initio* EXAFS code FEFF 5.[47] In the course of nonlinear least-squares curve fitting between the experimental spectrum and the theoretical one, the coordination number (N_i) was fixed to the crystallographically plaucible integer, and the other structural parameters such as the bond distance (R_i), the Debye−Waller factor (σ_i^2), and the threshold energy difference (ΔE_0) were optimized as variables. The amplitude reduction factor (S_0^2) was set equal to 0.9 in the entire course of fitting procedure.[41]

Structural Aspects

The crystal structure of $[Cu(C_4H_6N_2)_2](ClO_4)_2$ is triclinic with the space group $P\bar{1}$, where ethylenediamine ligands coordinate to form an approximately square coplanar structure with the methylene groups of the ligand occupying a gauche configuration, and the axial positions are occupied by oxygen atoms from the perchlorate anions.[42] The equatorial Cu−N bond lengths in the ethylenediamine ring are 2.03 and 2.05 Å, and the axial Cu−O bond distance is 2.60Å. The crystal system of $[Cu(C_{10}H_{24}N_4)](ClO_4)_2$ is also triclinic with the space group $P\bar{1}$.[43] The coordination sphere of the copper ion is defined by a planar arrangement of the four nitrogen atoms in the macrocyclic ligand with oxygen atoms from the perchlorate groups lying above and below this plane. The resulting tetragonally distorted octahedron gives the interatomic distances of Cu−N with 2.02(3) and 2.02(4) Å and Cu−O of 2.57(4) Å. Consequently, both Cu complexes are very similar in their local structures around the Cu ion.

Montmorillonite belongs to the group of two-dimensional layer silicates known as smectite minerals.[44] Each layer is composed of a sheet of aluminum or magnesium octahedra sandwiched between two sheets of SiO_4 tetrahedra (2:1 layer silicate), which has a unit cell structure consisting of 20 oxygen atoms and 4 OH groups. Such 2:1 layers are continuous in the a and b directions and are stacked one above the other in the c direction. In montmorillonite, isomorphous substitution of lower valent metal ion for Al^{3+} in the octahedral layer or for Si^{4+} in the tetrahedral one result in the formation of fixed negative charges on the layer lattice. Such a layer charge is balanced by interlayer cations such as Na^+ or Ca^{2+} in the interlamellar space, in which the water molecules or organic polar ones could be easily stabilized due to the high solvation enthalpy. The basal spacing can be, therefore, changed depending upon the nature of exchanged cations, the degree of solvation, and/or the size and geometry of the organic molecules. If the exchanged cation is a transition metal, the complex in the interlayer could be easily formed by reacting with electron-donating ligands. The coordination chemistry of the metal ion in the interlayer reaction field is often similar to that of the ion in solution, but it is frequently influenced in its behavior by the charge density and its distribution of the silicate layer.

Results and Discussion

X-ray Powder Diffraction. The intercalation of Cu^{2+}, $[Cu(en)_2]^{2+}$, and $[Cu(cyclam)]^{2+}$ ions into montmorillonite was confirmed by powder X-ray diffraction, in which (001) reflection

(40) Newville, M.; Livins, P.; Yacoby, Y.; Rehr, J. J.; Stern, E. A. *Phys. Rev. B* **1993**, *47*, 14126.

(41) Rehr, J. J.; Mustre de Leon, J.; Zabinsky, S. I.; Albers, R. C. *J. Am. Chem. Soc.* **1991**, *113*, 5135. Mustre de Leon, J.; Rehr, J. J.; Zabinsky, S. I. *Phys. Rev. B* **1991**, *44*, 4146. O'Day, P. A.; Rehr, J. J.; Zabinsky, S. I.; Brown, G. E., Jr. *J. Am. Chem. Soc.* **1994**, *116*, 2938.

(42) Pajunen, A. *Suomen Kem.* **1967**, *40*, 32.

(43) Tasker, P. A.; Sklar, L. *J. Cryst. Mol. Struct.* **1975**, *5*, 329.

(44) Brindley, C. W.; Brown, C. *Crystal Structures of Clay Minerals and their X-ray Identification*; Mineral Society: London, 1980.

(45) Slade, P. G.; Stone, P. A.; Radoslovich, E. W. *Clays Clay Miner.* **1985**, *33*, 51.

(46) Suzuki, M.; Yeh, M.; Burr, C. R.; Whittingham, M. S.; Koga, K.; Nishihara, H. *Phys. Rev. B* **1989**, *40*, 11229.

(47) Sham, T. K. *Acc. Chem. Res.* **1986**, *19*, 99.

Table 2. Structural Parameters Obtained from the Best Fit for the Cu K-Edge EXAFS Spectra

compound	atom	CN[a]	R^b (Å)	σ^{2c} ($\times 10^{-3}$/Å^2)	$E_0{}^d$ (eV)	crystallographic data (Å)
$[Cu(en)_2](ClO_4)_2$	N	4	2.02	5.9	2.3	2.03,[e] 2.05[e]
	O	2	2.53	16.5		2.60[e]
	C	4	2.84	11.0		
$[Cu(cyclam)](ClO_4)_2$	N	4	2.01	4.3	0.5	2.02(3),[f] 2.02(4)[f]
	O	2	2.52	14.6		2.57(4)[f]
	C	4	2.80	3.5		
	C	4	2.97	4.4		
	C	2	3.38	0.8		
$[Cu(H_2O)_4]^{2+}$−montmorillonite	O	4	1.93	4.0	−0.1	1.92[g]
$[Cu(en)_2]^{2+}$−montmorillonite	N	4	2.02	3.3	3.3	
	C	4	2.86	8.8		
$[Cu(cyclam)]^{2+}$−montmorillonite	N	4	2.01	3.5	3.2	
	C	4	2.85	5.4		
	C	4	3.00	4.9		
	C	2	3.39	3.4		

[a] Coordination number. [b] Distance. [c] Debye−Waller factor. [d] Threshold energy difference. [e] From refs 42 and 56. [f] From ref 43. [g] From ref 33. This value was obtained by EXAFS analysis.

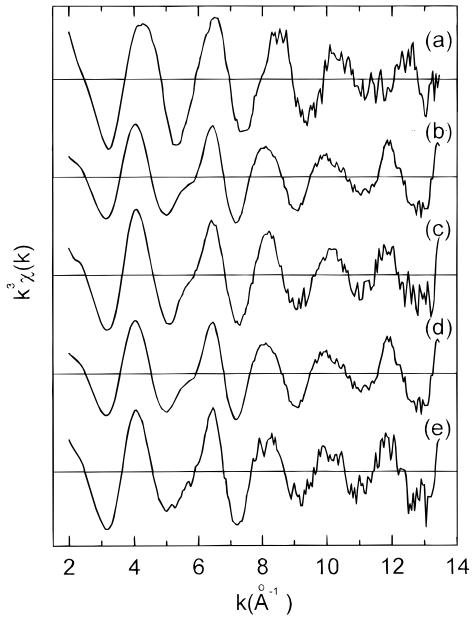

Figure 2. Cu K-edge EXAFS oscillations, $k^3\chi(k)$, for (a) $[Cu(H_2O)_4]^{2+}$−M, (b) $[Cu(en)_2](ClO_4)_2$, (c) $[Cu(en)_2]^{2+}$−M, (d) $[Cu(cyclam)](ClO_4)_2$, and (e) $[Cu(cyclam)]^{2+}$−M, where M indicates montmorillonite.

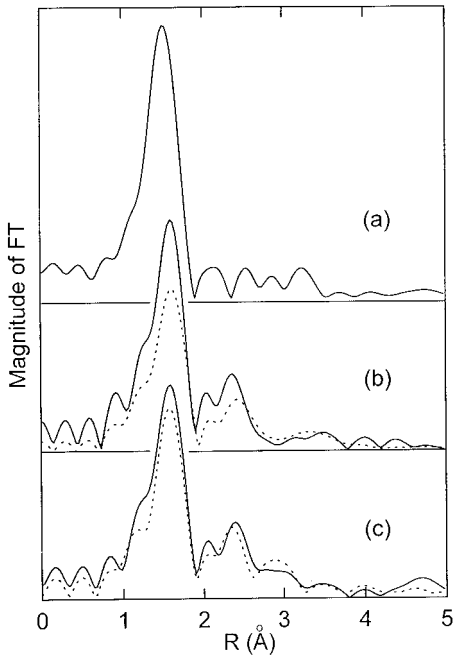

Figure 3. Magnitudes of Fourier transforms in the range of ∼2 Å^{-1} < k < ∼13 Å^{-1} of the Cu K-edge EXAFS oscillations, $k^3\chi(k)$, for (a) $[Cu(H_2O)_4]^{2+}$−M, (b) $[Cu(en)_2](ClO_4)_2$ (- - -), $[Cu(en)_2]^{2+}$−M (—), and (c) $[Cu(cyclam)](ClO_4)_2$ (- - -), $[Cu(cyclam)]^{2+}$−M (—), where M indicates montmorillonite.

appeared at $2\theta = 6.999°$ ($d = 12.618$ Å), 6.830° ($d = 12.932$ Å), and 6.560° ($d = 13.463$ Å), respectively. The observed basal increment ($\Delta d = 3.018$, 3.332, and 3.863 Å) with respect to the basal spacing of the pristine montmorillonite ($d = 9.60$ Å) suggests that the copper complex ions are intercalated as a monolayer with their square planes parallel to the silicate layers, and the axial ligands have been replaced by silicate lattices.

Cu K-Edge EXAFS Spectroscopy. Figures 2 and 3 show the Cu K-edge EXAFS oscillations, $\chi(k)$ weighted by k^3, and their FTs (FTs) in the range of ∼2 Å^{-1} < k < ∼13 Å^{-1}, respectively. It is clearly seen in FTs of Figure 3a that the Cu^{2+} ion−montmorillonite exhibits only the first intense peaks at ∼1−2 Å, corresponding to the interactions between the copper ions and oxygen atoms in the first coordination sphere. This implies that the copper ion in the Cu^{2+} ion−montmorillonite is not directly coordinated with the oxygen in the layer surface as an axial ligand, having only the four equatorial oxygen atoms, which could not be well discerned by other previous work using analytical techniques such as diffraction, IR, and EPR. While $[Cu(en)_2](ClO_4)_2$, $[Cu(cyclam)](ClO_4)_2$, and their intercalates exhibit more distant peaks up to ∼3 Å corresponding to the outer Cu−O and/or Cu···C shells besides the first peak due to the square planar Cu−N interaction in Figure 3b and c. In addition, another interesting feature in FTs is that both the intercalated copper complexes show the larger intensity in the first peak than their free copper complexes.

For quantitative analysis of the structural data, a nonlinear least-squares curve fitting was carried out on the FTs, using the UWXAFS code as described in the Experimental Section. For the Cu^{2+} ion−montmorillonite, a curve fitting was performed in the region of $R \leq 2.5$ Å corresponding to the distance from the copper to the nearest oxygen. With the coordination number (CN) of 4, the fitted Cu−O distance and the Debye−Waller factor are estimated to be 1.93 Å and 0.0041 Å^2, respectively, as shown in Table 2. These values are found to be very reasonable, and especially the bond distance is in good agreement with the previous EXAFS result for Cu−clay.[33] For both the copper complexes of $[Cu(en)_2](ClO_4)_2$ and $[Cu(cyclam)](ClO_4)_2$ the multishell fittings were performed in the region of 1 Å < R < 3.3 Å to obtain the local structural parameters, because contributions of the axial Cu−O bonds and the nonbonded Cu···C interactions as well as the equatorial

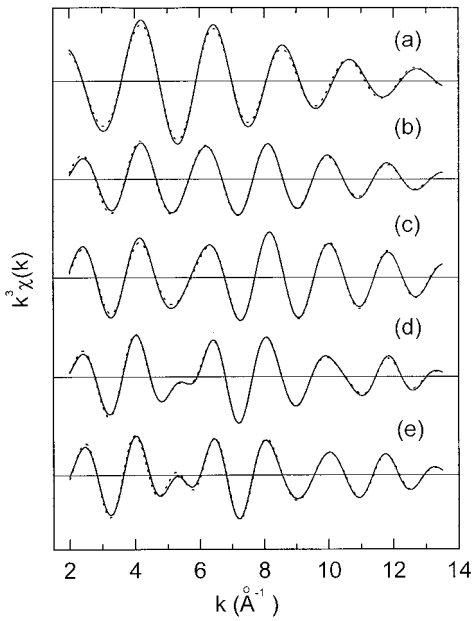

Figure 4. Comparisons between the experimental (—) and the theoretical inverse Fourier transforms, $k^3\chi(k)$, (- - -) for (a) $[Cu(H_2O)_4]^{2+}$—M, (b) $[Cu(en)_2](ClO_4)_2$, (c) $[Cu(en)_2]^{2+}$—M, (d) $[Cu(cyclam)](ClO_4)_2$, and (e) $[Cu(cyclam)]^{2+}$—M, where M indicates montmorillonite.

Cu—N bonds to EXAFS oscillation significantly interfere with one another so that each contribution to EXAFS oscillation could not be well resolved. But the number of refined variables (N_{var}) are limited to $N_{var} = 2 + (2\Delta k\Delta R)/\pi$, where Δk and ΔR indicate the analyzed k and R range, respectively. In the present case, the maximum number of refined variables is constrained to 11. Therefore, for the reliability of EXAFS analysis, it was assumed that EXAFS oscillations are composed of three or four shells with the Cu—N (CN = 4), Cu—O (CN = 2), and Cu···C (CN = 4) distances for $[Cu(en)_2](ClO_4)_2$, and Cu—N (CN = 4), Cu—O (CN = 2), Cu···C (CN = 4), and Cu···C (CN = 2) distances for $[Cu(cyclam)](ClO_4)_2$. The best-fitted structural parameters are presented in Table 2, and the inverse FTs, $k^3\chi(k)$, of the fitted regions on FTs are compared with the theoretical spectra depicted by using the obtained parameters in Figure 4. The best-fitted distances are shown to be in good agreement with the crystallographically determined distances within the experimental error limit (±0.02 Å). When EXAFS spectra for both the copper complexes intercalated into montmorillonite were analyzed in the same manner as their free complexes, however, we could not obtain reasonable parameters, which was revealed to be attributed to the presence of a Cu—O bonding pair. Therefore, the fittings were tried several times without the contribution of oxygen until physically meaningful results and best fits could be obtained. These fitted structural parameters are compared with those derived from the free copper complexes in Table 2, and the $k^3\chi(k)$ of the fitted regions on FTs are compared with the theoretical spectra depicted by using the obtained parameters in Figure 4. From these EXAFS analyses, it is clearly understood that the average Cu—N and Cu···C distances for the free copper complexes are hardly changed by their intercalation. But it should be noted that the copper ions in the copper complex—montmorillonite system do not have any axially coordinated oxygens, which is the same result as found in the copper ions intercalated into montmorillonite as mentioned above.[33] Considering the in-plane structure of the host silicate sheet in montmorillonite, two possible sites are available for the intercalated cation; one site is located between triangular basal oxygen atoms of the SiO_4 tetrahedra, and the other is the ditrigonal cavity often described as a siloxane ring.[45,46] The former site is known to be energetically favorable for small cations, and the latter for larger ones. On the basis of our experimental results, it is concluded that negatively charged layers are likely to act as axial counter anions, and the copper complex ions are stabilized at the center of siloxane ring consisting of montmorillonite as illustrated in the schematic arrangement of the copper complexes within the silicate layer (Figure 1b).

In addition, the Debye—Waller factor of the Cu—N bond for the copper complex—montmorillonite significantly decreases compared to those for the free complexes, despite the invariance of the average Cu—N bond distance. The Debye—Waller factor, which is one of the important variables in the EXAFS analysis, corresponds to the mean square relative displacement (MSRD) of the equilibrium of the Cu—N bond distance due to the dynamic (vibrational) and/or the static disorder.[47] Therefore a larger bond distance as well as a weaker bond strength results in a larger Debye—Waller factor due to the stronger thermal vibration, and the presence of static disorder owing to the defect structure or multiple bond distances also induces a larger Debye—Waller factor. Therefore, the decrease in the Debye—Waller factor of the Cu—N bond within the montmorillonite layers implies that the Cu—N bond distance becomes more regular and/or the bond covalency becomes more enhanced, compared to the cases of free complexes. In order to obtain more precise information from the value of the Debye—Waller factor, it is necessary to compare the crystallographic and EXAFS data. According to the previously reported crystallographic data for both free complexes,[42,43] there are two Cu—N bond distances with a difference of 0.02 Å for $[Cu(en)_2](ClO_4)_2$, whereas $[Cu(cyclam)](ClO_4)_2$ has almost the same Cu—N bond distance. And such a discrepancy in Cu—N bond distances is well reflected by the fact that the Debye—Waller factors obtained by the EXAFS analyses exhibit larger variation for the ethylenediamine complexes than for the cyclam ones. On the basis of both crystallographic and EXAFS data, the decreased Debye—Waller factors upon intercalation of the copper cyclam complex are mainly due to the decreased thermal vibration, resulting from the enhanced covalency in the Cu—N bonding rather than the more regular bond distances. But in case of the copper ethylenediamine complexes, it seems to be difficult to conclude only from the EXAFS result which of the above two effects mainly affects the decreased Debye—Waller factor upon intercalation. Variation of bond covalency will influence the bond distance and the electronic structure of central metal ion. Considering the experimental error limit (±0.02 Å) for the bond distance to be determined by EXAFS analysis, however, it is necessary to carefully examine how the change of the electronic structure upon the variation of bond covalency affects on the XANES spectra.

Cu K-Edge XANES Spectroscopy. Figure 5 shows the normalized Cu K-edge XANES spectra for the present compounds. Although each XANES spectrum exhibits a characteristic feature of a square-planar coordinated copper(II) ion with oxygen ligands[33,48] or nitrogen ones,[49,50] the spectra for copper ions with nitrogen ligands show the clear difference from that for the copper ions with oxygen ligands. But interpretation of the XANES spectrum is quite complicated, and thus conflicting assignments have been hitherto given for XANES spectra of transition metal compounds, despite various kinds of copper

(48) Garcia, J.; Benfatto, M.; Natoli, C. R.; Bianconi, A.; Fontaine, A.; Tolentino, H. *Chem. Phys.* **1989**, *132*, 295.
(49) Smith, T. A.; Penner-Hahn, J. P.; Berding, M. A.; Doniach, S.; Hodgson, K. O. *J. Am. Chem. Soc.* **1985**, *107*, 5945.
(50) Wakita, H.; Yamaguchi, T.; Yoshida, N.; Fujiwara, M. *Jpn. J. Appl. Phys.* **1993**, *32* (Suppl. 2), 836.

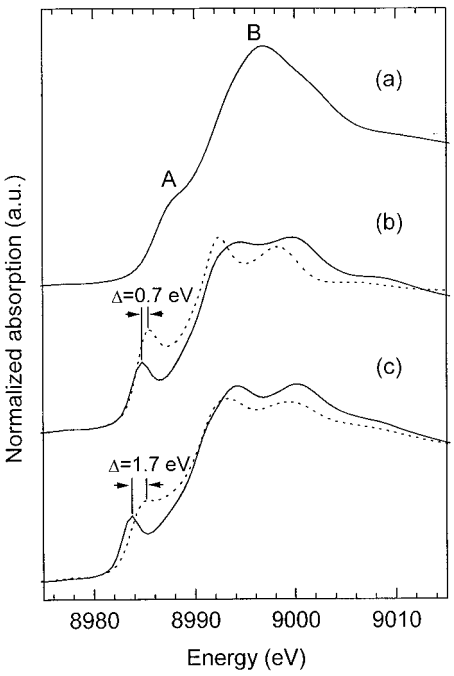

Figure 5. Normalized Cu K-edge XANES spectra for for (a) $[Cu(H_2O)_4]^{2+}$−M (−−), (b) $[Cu(en)_2](ClO_4)_2$ (- - -), $[Cu(en)_2]^{2+}$−M (−−), and (c) $[Cu(cyclam)](ClO_4)_2$, (- - -), $[Cu(cyclam)]^{2+}$−M (−−), where M indicates montmorillonite.

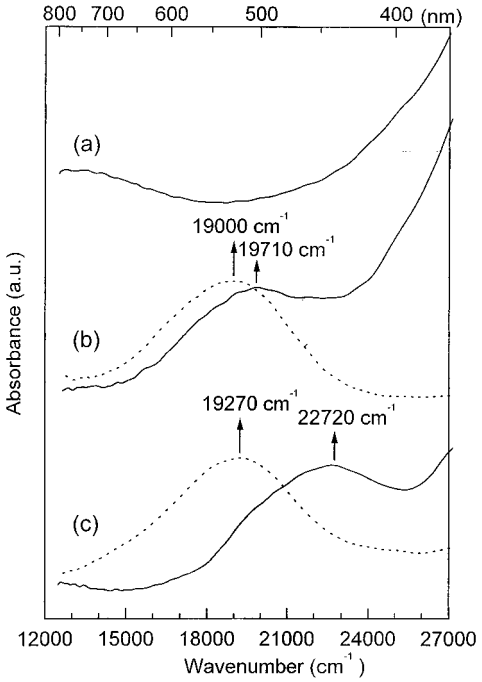

Figure 6. UV−visible spectra for (a) $[Cu(H_2O)_4]^{2+}$−M (−−), (b) $[Cu(en)_2](ClO_4)_2$ (- - -), $[Cu(en)_2]^{2+}$−M (−−), and (c) $[Cu(cyclam)](ClO_4)_2$, (- - -), $[Cu(cyclam)]^{2+}$−M (−−), where M indicates montmorillonite.

compounds having been extensively investigated to determine the correlation between edge features and the ligand filed geometry. For these reasons, it is not easy to assign all the peaks of the present XANES spectra in detail. But the main peak B can be assigned to the 1s → 4p transition, based on the dipole selection rule of $\Delta l = \pm 1$, and especially the shoulder peak A could be definitely assigned to the shakedown satellite involving a 1s → $4p_\pi$ transition with simultaneous ligand-to-metal charge transfer (LMCT) by means of the Cu K-edge XANES studies[51−54] for chemically well-characterized copper compounds. That is, the core hole final state is stabilized by additional screening due to the electron transfer from ligand p orbital to metal d orbital so that the dipolar transition can occur at lower energy, compared to that occurring without the additional screening effect by the charge transfer. It is therefore expected that peak A will shift to lower energy as LMCT occurs more effectively. In these regards, it is of great interest to compare XANES spectra between the free copper complexes and their montmorillonite intercalates. The oxidation state of the copper ion was not changed by the ion-exchange intercalation reaction, since no overall spectral shift could be observed. But it is obvious that the position of peak A shifts to a lower energy site upon intercalation, indicating that the charge transfer from 2p orbitals of the nitrogen ligand to 3d orbitals of the copper metal occurs more effectively as stated above, and thus the Cu−N bonding character becomes more covalent. Moreover, whereas both the free copper complexes exhibit peak A at almost the same energy position (8985.5 eV for $[Cu(en)_2](ClO_4)_2$ and 8985.4 eV for $[Cu(cyclam)](ClO_4)_2$), the degree of lower shift of peak A upon intercalation is larger for the cyclam complex ($\Delta = 1.7$ eV) than for the ethylenediamine one ($\Delta =$ 0.7 eV).

(51) Choy, J. H.; Kim, D. K.; Hwang, S. H.; Demazeau, G. *Phys. Rev. B* **1994**, *50*, 16631. Choy, J. H.; Kim, D. K.; Hwang, S. H.; Park, J. C. *J. Am. Chem. Soc.* **1995**, *117*, 7556.
(52) Bair, R. A.; Goddard, W. A., III *Phys. Rev. B* **1980**, *22*, 2767.
(53) Kosugi, N.; Yokoyama, T.; Asakura, K.; Kuroda, H. *Chem. Phys.* **1984**, *91*, 249.
(54) Yokoyama, T.; Kosugi, N.; Kuroda, H. *Chem. Phys.* **1986**, *103*, 101.

It has been already pointed out from the above EXAFS analyses that the decreased Debye−Waller factor of the Cu−N bond in the $[Cu(cyclam)]^{2+}$−montmorillonite is mainly attributed to the decreased thermal vibration due to the enhanced covalent Cu−N bond, but the main effect on the decreased Debye−Waller factor is not clear for the case of ethylenediamine complexes. These changes of the Debye−Waller factor obtained in EXAFS analyses are consistent with the lower shift of peak A in XANES spectra. That is, in the case of cyclam complex, the intercalation into montmorillonite significantly enhances the covalent Cu−N bonding character, resulting in the decreased Debye−Waller factor of the Cu−N bond. On the other hand, in the case of the ethylenediamine complex, a relatively smaller red shift of peak A with a larger decrease of the Debye−Waller factor compared to the cyclam complex indicates that the main effect on the decreased Debye−Waller factor upon intercalation into montmorillonite is the regularity of Cu−N bond distances rather than the enhanced covalency of the Cu−N bond. Now we could have an idea that the previously reported stability of complexes on clay surfaces[20−24] is due to the enhanced covalent character of the bonding in the copper complexes, and the kind of ligands would significantly influence the stability of the copper complexes on the clay surfaces. Such facts suggest that the crystal field strength on the copper site can be more diversely controlled by virtue of the intercalation reaction into the materials consisting of a charged layer such as clay.

UV−Visible Spectroscopy. Comparisons of UV−visible absorption spectra for free copper complexes with those for their montmorillonite complexes (see Figure 6) also demonstrate that copper complexes are held intact within the montmorillonite interlayers. All samples are characterized by one band in the visible region. The positions of band maximum are 19 000, 19 270, 13 070, 19 710, and 22 720 cm^{-1} for $[Cu(en)_2](ClO_4)_2$, $[Cu(cyclam)](ClO_4)_2$, and $[Cu(H_2O)_4]^{2+}$−, $[Cu(en)_2]^{2+}$−, and $[Cu(cyclam)]^{2+}$−montmorillonites, respectively, those which can be adequately explained as a d−d transition of Cu^{2+} in the framework of the effective symmetry D_{4h}. Of course, the position of the band maximum might not be a very good

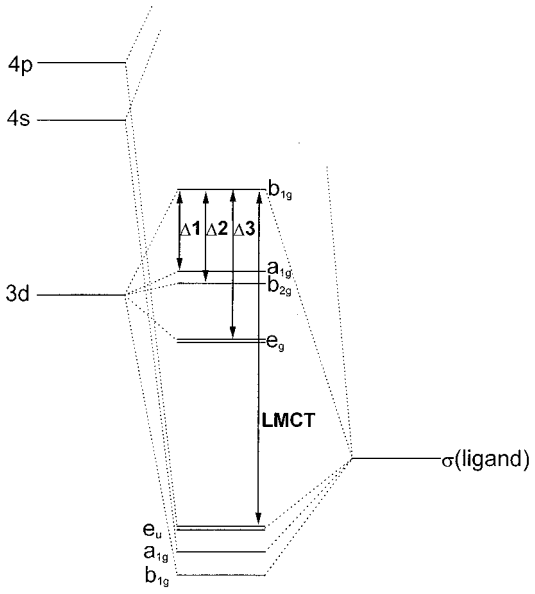

Figure 7. Qualitative molecular orbital energy diagram for the copper(II) complex in a D_{4h} crystal field.

parameter because a d−d transition in the visible region actually consists of three bands as shown in Figure 7. But the band maximum could represent the $^2E_g \rightarrow {}^2B_{1g}$ transition so that there is no problem in the qualitative comparison of the strength of the crystal field on the copper site. The present spectra for $[Cu(en)_2](ClO_4)_2$,[55−57] [Cu(cyclam)]$(ClO_4)_2$,[58] and $[Cu(H_2O)_4]^{2+}$−[27] and $[Cu(en)_2]^{2+}$−montmorillonites[22,24] are consistent with those previously reported. Interestingly, we can see that the positions of the d−d transition bands exhibit the same order as those of the A peaks in Cu K-edge XANES spectra. Figure 8 clearly shows that there is some correlation between the positions of d−d transition bands in UV−visible spectra and the A peaks in XANES spectra. These facts suggest that the effective charge transfer from the ligands to the copper ion gives rise to a large crystal field stabilization energy (CFSE) and thus enhanced stabilization of the copper complexes on clay surfaces. In this situation, it is necessary to note that the strong ligand field in the square-planar symmetry induces the destabilization of the antibonding $d_{x^2-y^2}$ orbital, and thus the change from square-planar Cu(II) with $3d^9$ electronic configuration to square-planar Cu(III) with $3d^8$ low-spin one is strongly favored by a large CFSE contribution.[7] Although the growing awareness that the redox reaction of Cu(II)−Cu(III) couple plays an important role in the catalytic reactions has invoked the electrochemical studies on the copper(II) complexes with various macrocyclic ligands, there is a paucity of comparable data for complexes with higher valent copper due to their instabilities. Therefore,

(55) Yamada, S.; Tsuchida, R. *Bull. Chem. Soc. Jpn.* **1956**, *29*, 289.
(56) Procter, I. M.; Hathaway, B. J.; Nicholls, P. *J. Chem. Soc. A* **1968**, 1678.
(57) Fujita, T.; Ohtaki, H. *Bull. Chem. Soc. Jpn.* **1983**, *56*, 3276.
(58) Amundson, A. R.; Whelan, J.; Bosnick, B. *J. Am. Chem. Soc.* **1977**, *99*, 6730.

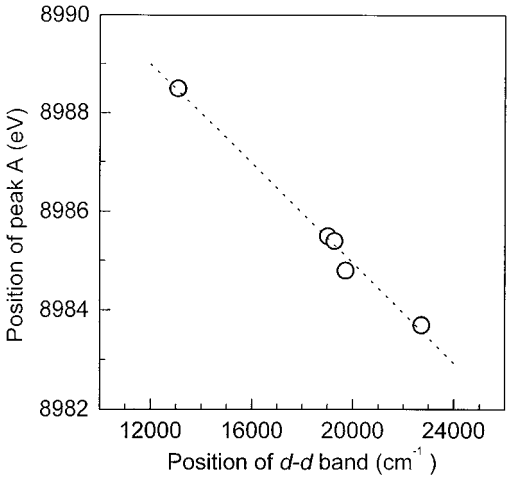

Figure 8. Positions of the d−d transition band in UV−visible spectra versus those of peaks A in XANES spectra.

the very large CFSE advantage of the copper complexes in the charged interlayer is expected to be able to stabilize Cu(III).

Conclusion

It was described that the X-ray absorption spectroscopic method is usefully applicable for examining the electronic structure as well as interlamellar structures of copper complexes in clay layers. EXAFS analyses at the Cu K-edge have shown that the copper ions within montmorillonite layers are not directly bonded to the layer oxygens, and the square-planar structures of copper complexes are not nearly changed upon the intercalation. From the changes of the Debye−Waller factor and the position of peak A in the Cu K-edge EXAFS and XANES spectra, it can been concluded that the origin of stabilizing the copper complex in montmorillonite is mainly due to the effective charge transfer from ligand to copper via out-of-plane π bonding. These X-ray absorption spectroscopic results could be also supported by the variations of the d−d transition band in the UV−visible spectra. In addition, a good linear correlation between the peak A positions and the d−d transition band position could be successfully demonstrated that the charge transfer is in some quantitative relation to the crystal field stabilization energy.

It is worth noting that the degree of the enhanced stability of the copper complex in the interlayer space of montmorillonite depends on the kind of ligand as shown in the case of the cyclam−montmorillonite intercalation complex. And it is also expected that the stability of copper complexes can be controlled through intercalation into various kinds of clay with different layer charges.

Acknowledgment. This research was in part supported by the Ministry of Education (Grant BSRI-96-3413) and by the Center for Molecular Catalysis (CMC). We thank Prof. M. Nomura for assistance during the XAS measurements.

IC960631N